Inorg. Chem. **2004**, *43*, 7042–7049

Inorganic Chemistry
Article

Preparation and Characterization of Novel Inorganic–Organic Hybrid Materials Containing Rare, Mixed-Halide Anions of Bismuth(III)

Andrea M. Goforth,[†] Mark D. Smith,[†] LeRoy Peterson, Jr.,[‡] and Hans-Conrad zur Loye*,[†]

Department of Chemistry and Biochemistry, The University of South Carolina, 631 Sumter Street,
Columbia, South Carolina 29208, and Department of Chemistry, Francis Marion University,
Florence, South Carolina 29501

Received June 17, 2004

Three new hybrid inorganic–organic salts containing novel mixed haloanions of bismuth were synthesized by the solvothermal reaction of bismuth iodide with a haloacid, HX ($X = Cl$ or Br), and the alkylamine 4,4′-trimethylenedipiperidine (TMDP). All three compounds were structurally characterized by single-crystal X-ray diffraction. Reaction of TMDP and BiI_3 with HCl yielded two crystalline products: $[H_2TMDP]_2[(Bi_2I_9)(BiCl_2I_2)]$ (**1**, major yield) and $[H_2TMDP]_2[Bi_2Cl_{10-x}I_x]$ (**2**, $x = 3.83$, minor yield). Compound **1** crystallizes in the monoclinic space group *Cc* ($a = 22.8586(11)$ Å, $b = 15.5878(7)$ Å, $c = 17.6793(9)$ Å, $\beta = 118.7010(10)°$, $Z = 4$) and contains the mononuclear mixed-halide anion $BiCl_2I_2^-$ in addition to a face-sharing bioctahedral $Bi_2I_9^{3-}$ anion and two independent H_2TMDP^{2+} cations. The $BiCl_2I_2^-$ anion has a sawhorse geometry (equatorially vacant trigonal bipyramidal geometry) that is not commonly observed in bismuth chemistry. Compound **2** crystallizes in the monoclinic space group $P2_1/c$ ($a = 14.9471(7)$ Å, $b = 12.7622(6)$ Å, $c = 13.3381(7)$ Å, $\beta = 116.1030(10)°$, $Z = 2$) and contains an edge-sharing bioctahedral mixed-halide anion in which iodide occupies one and chloride occupies two of the five crystallographically independent halide sites. The remaining two sites have mixed-chloride and -iodide occupancy. Reaction of TMDP and BiI_3 with HBr yielded the crystalline product $[H_2TMDP][BiBr_{5-x}I_x]$ (**3**, $x = 0.99$), which contains, in addition to the organic cation, a polymeric, mixed-haloanion of bismuth(III). Compound **3** crystallizes in the chiral, orthorhombic space group $P2_12_12_1$ ($a = 8.5189(5)$ Å, $b = 14.8988(9)$ Å, $c = 17.9984(11)$ Å, $Z = 4$) and consists of an H_2TMDP^{2+} cation in addition to the anion, which is built up of corner-sharing BiX_6 octahedra. Of the five crystallographically independent halide sites in this anion, two are occupied solely by Br and the remaining three have mixed-bromide and -iodide occupancy. Other anion stoichiometries have been observed crystallographically for **3**, as the specific stoichiometry is dependent on the relative concentration of the haloacid starting material used.

1. Introduction

The chemistry of the bismuth(III) halides has been explored for several decades owing to the strong tendency of bismuth to act as a halide ion acceptor.[1,2] Consequently, numerous complex haloanions of bismuth have been formed with a variety of cations, and these compounds have been found to exhibit a great deal of diversity in their structural and physical properties.[1−20]

Halobismuthate materials containing an organic countercation display extensive structural diversity, as the anion may be polymeric, discrete polynuclear, or mononuclear depend-

---

* Author to whom correspondence should be addressed. E-mail: zurloye@mail.chem.sc.edu. Phone: (803) 777-6916. Fax: (803) 777-8508.

[†] The University of South Carolina.

[‡] Francis Marion University, Florence.

(1) Cornia, A.; Fabretti, A. C.; Grandi, R.; Malavasi, W. *J. Chem. Crystallogr.* **1994**, *24*, 277.

(2) Clegg, W.; Errington, R. J.; Fisher, G. A.; Green, M. E.; Hockless, D. C. R.; Norman, N. C. *Chem. Ber.* **1991**, *124*, 2457.

(3) Geiser, U.; Wade, E.; Wang, H. H.; Williams, J. M. *Acta Crystallogr., Sect. C* **1990**, *46*, 1547.

(4) Lazarini, F. *Acta Crystallogr., Sect. C* **1987**, *43*, 875.

(5) Papavassiliou, G. C.; Koutselas, I. B.; Terzis, A.; Raptopoulou, C. P. *Z. Naturforsch., B: Chem. Sci.* **1995**, *50*, 1566.

(6) Robertson, B. K.; McPherson, W. G.; Meyers, E. A. *J. Phys. Chem.* **1967**, *71*, 3531.

(7) Zhu, X.-H.; Mercier, N.; Frere, P.; Blanchard, P.; Roncali, J.; Allain, M.; Pasquier, C.; Riou, A. *Inorg. Chem.* **2003**, *42*, 5330.

(8) Bigoli, F.; Lanfranchi, M.; Pellinghelli, M. A. *Inorg. Chim. Acta* **1984**, *90*, 215.

(9) Carmalt, C. J.; Farrugia, L. J.; Norman, N. C. *Z. Naturforsch., B: Chem. Sci.* **1995**, *50*, 1591.

(10) Chaabouni, S.; Kamoun, S.; Jaud, J. *J. Chem. Crystallogr.* **1997**, *27*, 527.

10.1021/ic049212d CCC: $27.50

ent upon the synthetic conditions employed. Conditions influencing the anion structure include the cation size and geometry, reaction temperature, reactant concentrations, and crystallization conditions.[1,2,9,11,14,20] The crystal packing in these materials is also quite varied and is directed by the interactions present between the components constituting the solid. Such interactions include van der Waals interactions, electrostatic interactions, hydrogen bonding, and anion−anion interactions provided by halide−halide contacts.[1,4,5,7,8,10,18] Many known halobismuthate compounds consist of one-dimensional, polymeric inorganic components separated from one another by organic species, and as a group, these materials are of interest as potential dimensionally restricted semiconductor materials.[12,13,16] Others have layered inorganic components[7,15,21] and may provide efficient routes to bismuth nanostructures, such as nanotubes and nanowires.[21] Finally, some compounds in this family are fully three-dimensional when weak interactions between components are considered.[8,10] Not surprisingly, the wide range of structural properties observed in these halobismuthate containing materials have motivated studies of their optical and electronic properties, including nonlinear optical activity, luminescence, and semiconductivity.[5,7,11,16]

Interestingly, bismuth halides have been used in the transhalogenation of alkyl halides,[22] where the bismuth containing product in such reactions is postulated to be a mixed-halide species. Despite the number and diversity of known halobismuthate materials, mixed halides of bismuth are comparatively rare. While mixed-halide species of phosphorus are numerous, the tendency to form mixed-halide species apparently decreases upon descending the group. To date, only a handful of mixed bismuth halides have been isolated and characterized, the majority of which have been mixed subhalides or aryl-mixed halides.[23,24] Other known mixed halides of bismuth include $[NEt_4][Bi(S_2CNEt_2)I_2Br]$,[25] $[EtMe_2PhN]_3[Bi_2Br_{8.70}I_{0.3}]$,[11] and $[C_2H_9N_4S]_3[BiCl_{5.67}I_{0.33}]$.[8] Herein, we wish to report the syntheses and single-crystal X-ray structures of three new inorganic−organic salts which contain mixed-halide anions of bismuth(III).

2. Experimental Section

2.1. Materials and Methods. BiI_3 (Alfa Aesar, 95%), 4,4′-trimethylenedipiperidine hydrate (TMDP·H_2O, Lancaster, 98+%), concentrated HCl (Fisher, ACS grade), and HBr (Acros, 33 wt % in glacial acetic acid) were purchased and used without further purification. Ethanol (AAPER, 100%) was used as received as the solvent for all syntheses. Powder X-ray diffraction experiments were performed on a Rigaku D/max 2200 diffractometer (Cu Kα radiation, $\lambda = 1.5418$ Å). Diffuse reflectance UV−visible spectroscopy (250−800 nm) was performed in absorbance mode on an Ocean Optics USB-2000 fiber optic spectrometer equipped with a standard reflection probe (200 μm read fiber). A poly(tetrafluoroethylene) diffuse reflectance standard (Ocean Optics WS-1) was used as the reference material.

2.1.1. Preparation of $[H_2TMDP]_2[(Bi_2I_9)(BiCl_2I_2)]$ (1) and $[H_2TMDP]_2[Bi_2Cl_{10-x}I_x]$ ($x = 3.83$) (2). BiI_3 (100.1 mg, 0.17 mmol) and TMDP·H_2O (27.3 mg, 0.12 mmol) were placed in a 23 mL Teflon-lined autoclave and covered with 6 mL of ethanol. Concentrated HCl (0.5 mL) was added dropwise to this mixture, and the autoclave was subsequently sealed. The autoclave was then heated at 1 °C/min to 140 °C and held at that temperature for 48 h. At the end of this period, the autoclave was cooled to 70 °C at 1 °C/min and held at this temperature for 6 h before cooling to room temperature at the same cooling rate. Red single crystals of **1** (major yield) and yellow single crystals of **2** (minor yield) were isolated directly from the reaction. A suitable single crystal of each was selected for X-ray crystallographic analysis. Crystals of the major phase (**1**) were separated from crystals of the minor phase (**2**) by hand-picking. Larger quantities of **2** may be obtained by increasing the relative concentration of HCl in the reaction (vide infra). Anal. Calcd for **1**: C, 12.40; H, 2.24; N, 2.22. Found: C, 12.82; H, 2.52; N, 2.00. Microanalytical data for the minor phase was not obtained, and the composition of the phase was determined solely from single-crystal X-ray diffraction measurement.

2.1.2. Preparation of $[H_2TMDP][BiBr_{5-x}I_x]$ ($x = 0.99$) (3). The preparation is the same as that used to prepare **1** and **2**, only 1 mL of HBr (33% in glacial acetic acid) was substituted for 0.5 mL of HCl. Yellow single crystals of **3** (57% yield based on BiI_3) were isolated directly from the reaction. A suitable single crystal was selected for X-ray crystallographic analysis. The remainder of the sample was shown to be phase pure by powder X-ray diffraction. Anal. Calcd for **3** ($x = 0.99$): C, 18.00; H, 3.25; N, 3.23. Found: C, 17.72; H, 3.03; N, 3.09.

Whereas **1** forms regardless of the amount of HCl added, the value of x in **3** is dependent on the amount of HBr added. For example, addition of 0.5 mL instead of 1 mL of HBr produced **3** with $x = 1.70$ but otherwise having the identical structure and similar unit cell parameters. For both **3** with $x = 0.99$ and **3** with $x = 1.70$, the value of x is determined solely from the single-crystal diffraction experiment.

2.1.3. Single-Crystal Structure Determinations. Suitable single crystals of **1**, **2**, and **3** were selected and mounted on the end of thin glass fibers using epoxy or an inert oil. X-ray intensity data were measured at 150.0(2) (**1**) or 293(2) K (**2**, **3**) on a Bruker SMART APEX CCD-based diffractometer (Mo Kα radiation, $\lambda = 0.71073$ Å).[26] Raw data frame integration and Lorentz-polarization corrections were performed with SAINT+.[26] Final unit cell parameters were determined by least-squares refinement of 8279, 4937, and 5542 reflections from the data sets of compounds **1**, **2**, and **3** respectively with $I > 5(\sigma)I$. Analysis of the data sets showed

---

(11) Eickmeier, H.; Jaschinski, B.; Hepp, A.; Nub, J.; Reuter, H.; Blachnik, R. *Z. Naturforsch., B: Chem. Sci.* **1999**, *54*, 305.

(12) Feldmann, C. *Inorg. Chem.* **2001**, *40*, 818.

(13) Geiser, U.; Wang, H. H.; Budz, S. M.; Lowry, M. J.; Williams, J. M.; Ren, J.; Whangbo, M.-H. *Inorg. Chem.* **1990**, *29*, 1611.

(14) Krautscheid, V. H. *Z. Anorg. Allg. Chem.* **1994**, *620*, 1559.

(15) Mitzi, D. B. *Inorg. Chem.* **2000**, *39*, 6107.

(16) Mousdis, G. A.; Papavassiliou, G. C.; Terzis, A.; Raptopoulou, C. P. *Z. Naturforsch., B: Chem. Sci.* **1998**, *53*, 927.

(17) Krautscheid, V. H. *Z. Anorg. Allg. Chem.* **1999**, *625*, 192.

(18) Kubiak, R.; Ejsmont, K. *J. Mol. Struct.* **1999**, *474*, 275.

(19) Mammano, N. J.; Zalkin, A.; Landers, A.; Rheingold, A. L. *Inorg. Chem.* **1977**, *16*, 297.

(20) Feldmann, C. *J. Solid State Chem.* **2003**, *172*, 53.

(21) Wang, J.; Li, Y. *Adv. Mater.* **2003**, *15*, 445.

(22) Boyer, B.; Kermane, E. M.; Arpin, S.; Montero, J.-L.; Roque, J.-P. *Tetrahedron* **1999**, *55*, 1971.

(23) Sharma, P.; Cabrera, A.; Rosas, N.; Arias, J. L.; Lemus, A.; Sharma, M.; Hernandez, S.; Garcia, J. L. *Z. Anorg. Allg. Chem.* **2000**, *626*, 921.

(24) Dikarev, E. V.; Popovkin, B. A.; Shevelkov, A. V. *Russ. Chem. Bull.* **2001**, *50*, 2304.

(25) Raston, C. L.; Rowbottom, G. L.; White, A. H. *J. Chem. Soc., Dalton Trans.* **1981**, 1369.

(26) *SMART*, Version 5.625; *SAINT+*, Version 6.02a; *SADABS*; Bruker Analytical X-ray Systems, Inc.: Madison, WI, 1998.

Table 1. Crystallographic Data for **1**, **2**, and **3**

compound	**1**	**2**	**3** ($x = 0.99$)
formula	$C_{26}H_{56}Bi_3Cl_2I_{11}N_4$	$C_{26}H_{56}Bi_2Cl_{6.17}I_{3.83}N_4$	$C_{13}H_{28}BiBr_{4.01}I_{0.99}N_2$
formula weight	2518.49	1547.46	867.42
crystal system	monoclinic	monoclinic	orthorhombic
space group	*Cc*	$P2_1/c$	$P2_12_12_1$
a (Å)	22.8586(11)	14.9471(7)	8.5189(5)
b (Å)	15.5878(7)	12.7622(6)	14.8988(9)
c (Å)	17.6793(9)	13.3381(7)	17.9984(11)
α (deg)	90	90	90
β (deg)	118.7010(10)	116.1030(10)	90
γ (deg)	90	90	90
volume (Å^3)	5524.4(5)	2284.83(19)	2284.4(2)
Z	4	2	4
ρ_{calc} (Mg m^{-3})	3.027	2.249	2.522
μ (mm^{-1})	15.796	10.662	16.067
temperature (K)	150.0(2)	293(2)	293(2)
reflections collected	21304	15775	19119
independent reflections	9659	3632	4055
goodness of fit	0.989	1.023	1.023
final *R* indices, [$I > 2\sigma(I)$]	R1 = 0.0328 wR2 = 0.0687	R1 = 0.0421 wR2 = 0.1008	R1 = 0.0248 wR2 = 0.0577
R indices, all data	R1 = 0.0367 wR2 = 0.0696	R1 = 0.0621 wR2 = 0.1094	R1 = 0.0270 wR2 = 0.0587

negligible crystal decay during collection. An empirical absorption correction based on multiple measurements of equivalent reflections was applied for each.[26]

For compound **1**, systematic absences in the intensity data were consistent with the space groups *C*2/*c* and *Cc*; intensity statistics followed an acentric distribution. The structure was solved in *Cc* by a combination of direct methods and difference Fourier syntheses and refined by full matrix least-squares against F^2, using SHELXTL.[27] Upon successful solution and refinement in *Cc*, a check for missed symmetry was performed with ADDSYM/PLATON,[28] which verified the space group choice. At convergence, the absolute structure (Flack) parameter was −0.009(4), confirming the correct absolute structure and the absence of inversion twinning. All non-hydrogen atoms were refined with anisotropic displacement parameters; hydrogen atoms were placed in geometrically idealized positions and included as riding atoms.

For compound **2**, systematic absences in the intensity data confirmed the space group $P2_1/c$. Direct methods structure solution, difference Fourier syntheses, and full matrix least-squares refinement against F^2 were performed with SHELXTL.[27] The asymmetric unit consists of half of a $[Bi_2Cl_{10-x}I_x]^{4-}$ anion located on a crystallographic inversion center and one complete $[C_{13}H_{28}N_2]^{2+}$ cation. After location of reasonable positions for all halide atoms of the anion, refinement of the unique two apical sites as single sites fully occupied by either Cl or I resulted in unreasonably large or small, and also significantly elongated, displacement parameters. These two sites were successfully modeled as split, mixed Cl/I positions. The affected halide sites are Cl3/I3 and I4/Cl4. For both split sites, the position further from Bi was assigned as iodine and the position closer to Bi as chlorine. Initially, occupancies for both were allowed to refine freely. The resulting occupancy sums were close to unity, thereby supporting the assignment as a mixed Cl/I position. For the final cycles, the occupancies were constrained to sum to unity. The final refined occupancies are Cl3/I3 0.792(4)/0.208(4) and I4/Cl4 0.707(4)/0.293(4). No unusual problems were encountered for Cl1, I1, or Cl2, and the final refined composition of the anion is then "$Bi_2Cl_{6.17}I_{3.83}$". All non-hydrogen atoms were refined with anisotropic displacement parameters; hydrogen atoms were placed in idealized positions and included as riding atoms.

For compound **3**, systematic absences in the intensity data uniquely determined the space group as $P2_12_12_1$. The structure was solved by a combination of direct methods and difference Fourier syntheses and refined by full matrix least-squares against F^2 (SHELXTL).[27] The asymmetric unit contains the $[C_{13}H_{28}N_2]^{2+}$ cation and the "$BiBr_4I$" inorganic chain repeat unit. All hydrogen atoms of the cation could be located in the difference map. For the final refinement, hydrogens were placed in geometrically idealized positions and included as riding atoms. Preliminary refinement of three of the five independent halides of the inorganic chain as fully occupied resulted in unreasonably large or small displacement ellipsoids when refined as either Br or I due to statistical Br/I disorder on these sites. The affected atoms are Br3, I1, and I2 (final labeling scheme). Site occupation factors for these mixed Br/I positions were refined subject to summing to unity. Positional and displacement parameters were held equal due to the fact that the atoms are too close in space to refine independently. The final refined occupancy ratios are Br3/I33 0.912(5)/0.088(5), I1/Br11 0.425(6)/0.575(6), and I2/Br22 0.477(7)/0.523(7). A fractional occupancy/vacancy model was not considered as this would violate charge neutrality. No unusual problems were observed for Br1 and Br2. The final refined composition is then "$BiBr_{4.01}I_{0.99}$". At convergence, the Flack parameter was −0.048(7). All non-hydrogen atoms were refined anisotropically; hydrogens were calculated and included as riding atoms.

A second crystalline compound, prepared in the same manner as **3** only using a smaller amount of HBr, was also examined by X-ray crystallography. Atomic coordinates from the previous crystal were used as an initial model for refinement, and the quick convergence confirmed the isostructurality of the two. In the second crystalline compound, the same three anion sites were found to be affected by Br/I mixing. Analogous refinement of these three positions resulted in occupancy ratios of Br3/I33 0.727(7)/0.273(7), I1/Br11 0.715(8)/0.285(8), and I2/Br22 0.708(8)/0.292(8). The final refined composition is then "$BiBr_{3.30}I_{1.70}$", and the absolute structure (Flack) parameter was −0.03(1). Non-hydrogen atoms were refined anisotropically, and hydrogen atoms were placed in idealized positions and included as riding atoms.

Details of the crystallography experiments for **1**, **2**, and **3** ($x = 0.99$) are given in Table 1. Table 2 lists important interatomic distances and angles for compounds **1**, **2**, and **3**. Fractional atomic coordinates for **1**, **2**, and **3** with $x = 0.99$ as well as for **3** with $x = 1.70$ are found in the Supporting Information.

---

(27) Sheldrick, G. M. *SHELXTL*, Version 5.1; Bruker Analytical X-ray Systems, Inc.: Madison, WI, 1997.

(28) Spek, A. L. *PLATON, A Multipurpose Crystallographic Tool*; University of Utrecht: Utrecht, The Netherlands, 1998.

Table 2. Interatomic Distances (Å) and Bond Angles (deg) for the Anions of **1**, **2**, and **3**

			Compound **1**				
			$[BiCl_2I_2]^-$				
Cl(1)−Bi(1)−Cl(2)	170.51(10)	I(1)−Bi(1)−I(2)	95.61(4)	Bi(1)−Cl(1)	2.667(3)	Bi(1)−I(1)	2.8165(11)
Cl(1)−Bi(1)−I(1)	87.09(8)	Cl(2)−Bi(1)−I(1)	85.53(7)	Bi(1)−Cl(2)	2.815(3)	Bi(1)−I(2)	2.8587(11)
Cl(1)−Bi(1)−I(2)	87.71(8)	Cl(2)−Bi(1)−I(2)	87.09(7)				
			$[Bi_2I_9]^{3-}$				
I(3)−Bi(2)−I(4)	95.55(3)	I(6)−Bi(2)−I(7)	86.10(3)	I(8)−Bi(3)−I(9)	167.11(3)	I(9)−Bi(3)−I(10)	96.14(4)
I(3)−Bi(2)−I(5)	95.36(3)	I(6)−Bi(2)−I(8)	82.18(3)	I(8)−Bi(3)−I(10)	93.25(3)	I(9)−Bi(3)−I(11)	96.57(3)
I(3)−Bi(2)−I(6)	85.30(3)	I(6)−Bi(3)−I(7)	86.71(3)	I(8)−Bi(3)−I(11)	91.97(3)	I(10)−Bi(3)−I(11)	91.54(3)
I(3)−Bi(2)−I(7)	89.57(3)	I(6)−Bi(3)−I(8)	81.81(3)				
I(3)−Bi(2)−I(8)	164.50(3)	I(6)−Bi(3)−I(9)	88.82(3)	Bi(2)−I(3)	3.0082(10)	Bi(3)−I(9)	2.9688(11)
I(4)−Bi(2)−I(5)	91.81(3)	I(6)−Bi(3)−I(10)	175.04(3)	Bi(2)−I(4)	2.9264(11)	Bi(3)−I(10)	2.9452(11)
I(4)−Bi(2)−I(6)	175.20(3)	I(6)−Bi(3)−I(11)	88.13(3)	Bi(2)−I(5)	2.8948(11)	Bi(3)−I(11)	2.9296(11)
I(4)−Bi(2)−I(7)	89.18(3)	I(7)−Bi(2)−I(8)	80.51(3)	Bi(2)−I(6)	3.2314(11)	Bi(3)−I(6)	3.2274(10)
I(4)−Bi(2)−I(8)	96.19(3)	I(7)−Bi(3)−I(8)	80.59(3)	Bi(2)−I(7)	3.2885(10)	Bi(3)−I(7)	3.2562(10)
I(5)−Bi(2)−I(6)	92.81(3)	I(7)−Bi(3)−I(9)	90.10(3)	Bi(2)−I(8)	3.2219(10)	Bi(3)−I(8)	3.2497(10)
I(5)−Bi(2)−I(7)	174.85(3)	I(7)−Bi(3)−I(10)	93.02(3)	Bi(2)···Bi(3)	4.1768(7)		
I(5)−Bi(2)−I(8)	94.35(3)	I(7)−Bi(3)−I(11)	171.48(3)				
			Compound **2**				
			$[Bi_2Cl_{6.17}I_{3.83}]^{4-}$				
Cl(1)−Bi(1)−Cl(2)	89.50(7)	Cl(2)−Bi(1)−I(1)	174.88(5)	Cl(3)−Bi(1)−I(1)	88.0(3)	I(1)−Bi(1)−I(3)	91.7(3)
Cl(1)−Bi(1)−Cl(2)^a	168.95(8)	Cl(2)−Bi(1)−I(3)	87.0(3)	Cl(3)−Bi(1)−I(4)	178.9(4)	I(1)−Bi(1)−I(4)	91.68(5)
Cl(1)−Bi(1)−Cl(3)	86.6(4)	Cl(2)−Bi(1)−I(4)	89.78(7)	Cl(4)−Bi(1)−I(1)	85.0(5)	I(3)−Bi(1)−I(4)	176.0(3)
Cl(1)−Bi(1)−Cl(4)	94.0(7)	Bi(1)−Cl(2)−Bi(1)^a	98.94(7)	Cl(4)−Bi(1)−I(3)	176.6(6)		
Cl(1)−Bi(1)−I(1)	95.34(6)	Cl(2)^a−Bi(1)−Cl(3)	87.7(4)				
Cl(1)−Bi(1)−I(3)	85.2(3)	Cl(2)^a−Bi(1)−Cl(4)	92.7(7)	Bi(1)−I(1)	2.9741(9)	Bi(1)−Cl(1)	2.630(2)
Cl(1)−Bi(1)−I(4)	92.39(9)	Cl(2)^a−Bi(1)−I(1)	93.95(5)	Bi(1)−I(3)	3.191(12)	Bi(1)−Cl(2)	2.843(3)
Cl(2)−Bi(1)−Cl(2)^a	81.06(7)	Cl(2)^a−Bi(1)−I(3)	88.6(3)	Bi(1)−I(4)	2.995(3)	Bi(1)−Cl(3)	2.740(10)
Cl(2)−Bi(1)−Cl(3)	90.6(3)	Cl(2)^a−Bi(1)−I(4)	93.31(8)	Bi(1)−Cl(2)^a	2.911(2)	Bi(1)−Cl(4)	2.87(4)
Cl(2)−Bi(1)−Cl(4)	96.4(5)	Cl(3)−Bi(1)−Cl(4)	173.0(6)	Bi(1)A−Cl(2)	2.911(2)	Bi(1)···Bi(1)^a	4.374(7)
			Compound **3**				
			$[BiBr_{4.01}I_{0.99}]^{2-}$				
I(1)−Bi−I(2)	92.86(2)	I(2)−Bi−Br(1)	172.07(2)	Br(1)−Bi−Br(1)^b	87.297(7)	Br(2)−Bi−Br(1)^b	85.64(2)
I(1)−Bi−I(33)	92.84(2)	I(2)−Bi−Br(1)^b	84.92(2)	Br(1)−Bi−Br(2)	85.48(2)	Bi−Br(1)^b−Bi^c	178.98(3)
I(1)−Bi−Br(1)	94.90(3)	I(2)−Bi−Br(2)	92.41(2)				
I(1)−Bi−Br(1)A	177.61(2)	I(33)−Bi−Br(1)	86.94(2)	Bi−I(1)	2.7740(7)	Bi−Br(1)	3.0448(8)
I(1)−Bi−Br(2)	93.60(2)	I(33)−Bi−Br(2)	170.45(2)	Bi−I(2)	2.8361(7)	Bi−Br(2)	2.8595(7)
I(2)−Bi−I(33)	94.32(3)	I(33)−Bi−Br(1)^b	88.20(2)	Bi−I(33)	2.8847(7)	Bi−Br(1)^b	3.1258(8)

[a−c] Symmetry transformations used to generate equivalent atoms: [a] $-x, -y + 1, -z$. [b] $x - {}^1/_2, -y + {}^3/_2, -z + 1$. [c] $x + {}^1/_2, -y + {}^3/_2, -z + 1$.

3. Results and Discussion

3.1. Syntheses. The bismuth(III) trihalides have remarkable halide ion acceptor properties as evidenced by the numerous, complex haloanions of bismuth(III) that have been reported in the literature. Frequently, additional halide ions are supplied to BiX_3 by alkylammonium or arylammonium halide salts,[3,25,9,11] and these additional halide ligands are thought to terminate Bi−X−Bi linkages in the extended array of solid BiX_3, thereby affecting a reduction in dimensionality.[29] Additionally, the organic cation of the halide salt is typically incorporated into the product to provide charge balance for the bismuth haloanion formed by uptake of X^-.

An alternate synthetic route to halobismuthate materials involves the reaction of BiX_3 with an alkylamine, which can be protonated under the reaction conditions to serve as the charge balancing cation, and a haloacid (HX), which serves both as a source of X^- to terminate Bi−X−Bi bridges and as a proton donor. We have determined that the latter route can provide an effective synthetic pathway to mixed haloanions of bismuth when the bismuth trihalide and the haloacid starting materials do not contain the same halogen.

Using this route and employing BiI_3, trimethylenedipiperidine (TMDP), and HX (X = Cl, Br) as starting materials, we succeeded in the synthesis of three new halobismuthate materials. When HCl is used as the haloacid starting material, red single crystals of **1** and yellow single crystals of **2** are obtained. The former contains a mononuclear, mixed haloanion of bismuth, namely, the $BiCl_2I_2^-$ anion. The anionic component in the latter is a dinuclear mixed haloanion of bismuth with the empirical formula $[Bi_2Cl_{6.17}I_{3.83}]^{4-}$, where deviations from whole number stoichiometries are caused by statistical mixing of Cl and I on some of the independent halide sites (see structure determination). While compound **1** is always observed under these reaction conditions, larger quantities of compound **2** can be obtained by using greater relative quantities of the HCl starting material. By contrast, when HBr is used as the haloacid starting material, the anionic component is always a polymeric mixed haloanion of bismuth(III) with the general formula $BiBr_{5-x}I_x$, where x is dependent upon the relative amount of HBr employed in the synthesis. As expected, use of greater relative quantities of HBr results in the anion having a higher Br content than when smaller amounts are employed.

The reaction of BiI_3 and TMDP with HF was also attempted under synthetic conditions similar to those employed to obtain compounds **1**, **2**, and **3**. However, no mixed fluoride/iodide compound of bismuth was observed. This observation is consistent with the preference of bismuth(III), which is generally regarded as a soft acid,[22] for softer ligands.

---

(29) Tulsky, E. G.; Long, J. R. *Chem. Mater.* **2001**, *13*, 1149.

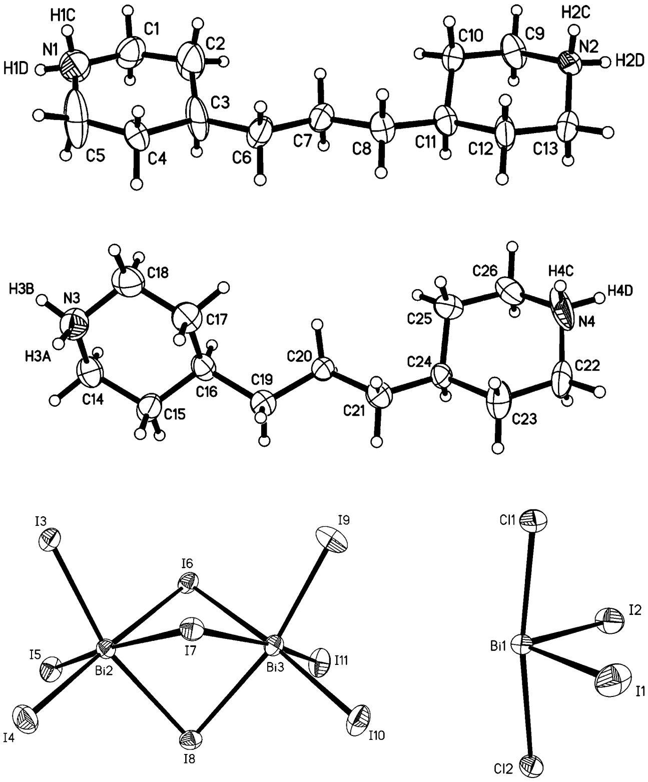

Figure 1. Ellipsoid plots of the components of $[H_2TMDP]_2[(Bi_2I_9)(BiCl_2I_2)]$ (**1**). Displacement ellipsoids are drawn at the 50% probability level. The two independent $[H_2TMDP]^{2+}$ cations (top and middle), the $Bi_2I_9^{3-}$ anion (bottom left), and the $BiCl_2I_2^-$ anion (bottom right) are shown.

3.2. Structural Discussion. 3.2.1. Compound 1. The compound $[H_2TMDP]_2[(Bi_2I_9)(BiCl_2I_2)]$ (**1**) is composed of two crystallographically independent, protonated TMDP cations and two different haloanions of bismuth(III), $Bi_2I_9^{3-}$ and $BiCl_2I_2^-$. The $Bi_2I_9^{3-}$ anion, which is constituted of two face-sharing BiI_6 octahedra, is commonly observed in bismuth iodide chemistry. Bond distances and angles for this anionic component of compound **1** are given in Table 2 and are similar to those determined for other compounds containing the $Bi_2I_9^{3-}$ anion.[11,4,7]

On the other hand, the $BiCl_2I_2^-$ anionic component has, to the best of our knowledge, never been reported in the literature. Figure 1 shows the ORTEP diagram of the $BiCl_2I_2^-$ anion, where it is readily apparent that the coordination geometry about bismuth(III) is distorted trigonal bipyramidal with a vacant equatorial ligand site. While an octahedral arrangement of halide ligands about bismuth(III) is by far the most frequently occurring geometry in bismuth halide chemistry, examples of square pyramidal (e.g., $(Bzl_4P)_2[Bi_2I_8]$ (Bzl = $-CH_2-C_6H_5$);[17] $(Bu_4N)_2[Ph_2Bi_2Cl_4Br_2]$ and $(Bu_4N)_2[Ph_2Bi_2Br_4I_2]$;[23] and $(Bu_4N)_2[Bi_2Ph_2Br_6]$[30]) and equatorially vacant trigonal bipyramidal bismuth(III) halide compounds (e.g., $(NEt_4)[BiPh_2I_2]$))[30] have been reported previously. In the case of the $BiCl_2I_2^-$ anion reported here, it is probable that the unusual coordination geometry results from the localization of the $6s^2$ lone pair (E) electron density. Thus, an AX_4E coordination environment results in the equatorially vacant trigonal bipyramidal shape. This suggestion is supported by the observation that the less sterically demanding chloride ligands are both found in the axial positions (Cl(1)−Bi(1)−I(1) = 87.09(8)°; Cl(1)−Bi(1)−I(2) = 87.71(8)°) while the bulkier iodide ligands are both located in the equatorial positions (I(1)−Bi(1)−I(2) = 95.61(4)°). Bond distances and angles for the $BiCl_2I_2^-$ anion are also found in Table 2.

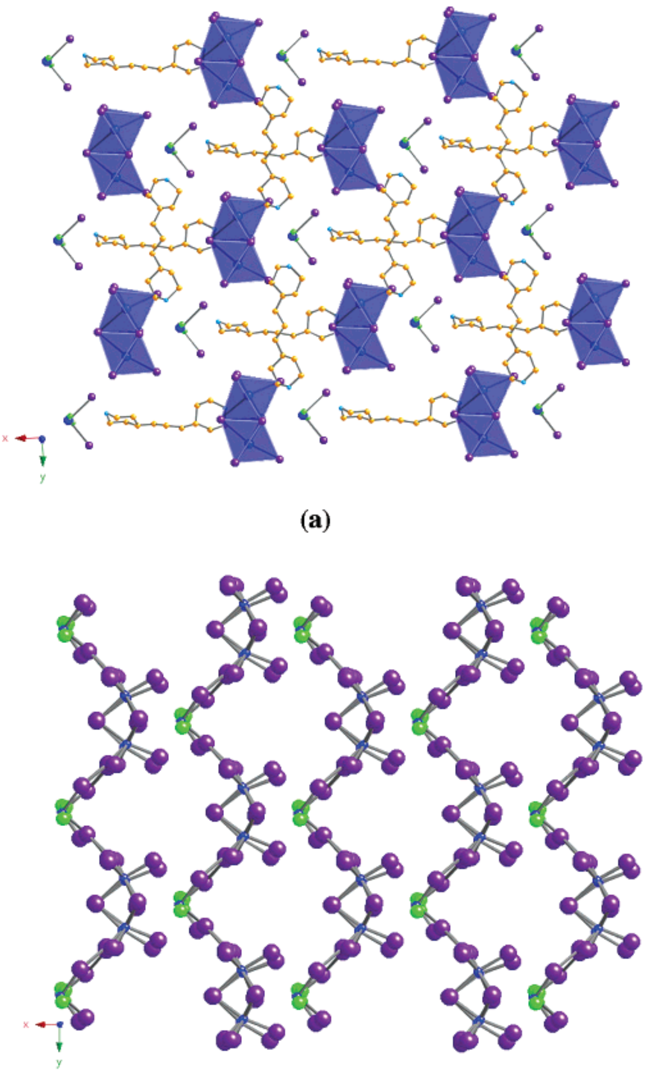

(a)

(b)

Figure 2. (a) (001) view of the crystal packing in $[H_2TMDP]_2[(Bi_2I_9)(BiCl_2I_2)]$ (**1**). Bi polyhedra are shown in blue; C, yellow; N, pale blue; I, purple; Cl, green. (b) (001) view of **1** highlighting the halide−halide interactions. Cl···Cl interactions are parallel to 001; cations are omitted for clarity.

The crystal packing in **1** along the crystallographic *c*-axis is shown in Figure 2a. Several hydrogen bonding interactions between the protonated cations and both anions are responsible for the observed arrangement of the components. It is worth noting that the H_2TMDP cation is conformationally flexible owing to the trimethylene spacer between the piperidyl rings, and it is this flexibility that allows for the multiple hydrogen bonding interactions in the solid. The details of the hydrogen bonding interactions present in **1** are summarized in Table 3.

---

(30) Clegg, W.; Errington, R. J.; Fisher, G. A.; Flynn, R. J.; Norman, N. C. *J. Chem. Soc., Dalton Trans.* **1993**, 638.

Table 3. Hydrogen Bond Distances (Å) and Angles (deg) for **1**

D−H···A	*d*(D−H)	*d*(H···A)	*d*(D···A)	∠(DHA)
N(1)−H(1C)···I(3)	0.92	3.04	3.893(18)	155.0
N(1)−H(1D)···Cl(2)	0.92	2.61	3.230(14)	125.6
N(1)−H(1D)···Cl(1)[a]	0.92	2.66	3.426(16)	140.8
N(2)−H(2C)···I(9)[b]	0.92	2.85	3.715(12)	156.6
N(2)−H(2D)···Cl(2)[b]	0.92	2.55	3.291(11)	137.6
N(2)−H(2D)···Cl(1)[c]	0.92	2.58	3.285(12)	133.9
N(3)−H(3A)···I(11)[d]	0.92	3.10	3.801(13)	134.8
N(3)−H(3A)···I(6)[d]	0.92	3.22	3.874(13)	129.5
N(3)−H(3B)···I(7)[e]	0.92	3.02	3.770(12)	139.9
N(3)−H(3B)···I(4)[e]	0.92	3.17	3.829(13)	130.3
N(4)−H(4C)···I(10)[f]	0.92	2.93	3.800(15)	157.3
N(4)−H(4D)···Cl(2)[g]	0.92	2.31	3.199(13)	162.3

[a−g] Symmetry transformations used to generate equivalent atoms: [a] $x, -y, z - 1/2$ [b] $x, y + 1, z$ [c] $x, -y + 1, z - 1/2$ [d] $x - 1/2, y - 1/2, z$ [e] $x - 1/2, -y - 1/2, z + 1/2$ [f] $x, -y - 1, z + 1/2$ [g] $x + 1/2, y - 1/2, z + 1$.

As a result of the hydrogen bonding interactions, the two anionic components are brought into close contact and, consequently, several I···I interactions can be identified for **1** (Figure 2b). These I···I interactions fall in the range 3.6969(16) to 3.9553(16) Å and are slightly shorter than twice the iodine van der Waals radius (1.98 Å).[31] By way of comparison, long bonds in polyiodides fall into the range of 3.1−3.5 Å.[32] In addition to the I···I interactions, a weak Cl···Cl interaction (3.495 Å) can be identified between the chloride ligands of adjacent $BiCl_2I_2^-$ anions (Cl van der Waals radius is 1.75 Å).[31] The three I···I interactions connect the two anionic components of **1** into one-dimensional chains running along the [010] crystallographic direction, while the lone Cl···Cl interaction connects the anionic chains into sheets in the *yz* plane. Details of these halide−halide interactions are given in the Supporting Information.

3.2.2. Compound 2. The compound $[H_2TMDP]_2[Bi_2Cl_{6.17}I_{3.83}]$ (**2**) is composed of protonated TMDP cations and a dinuclear, mixed haloanion of bismuth(III). The anionic component, $(Bi_2Cl_{6.17}I_{3.83})^{4-}$ (Figure 3), is built up of two edge-sharing BiX_6 octahedral units resulting in a centrosymmetric $Bi_2X_{10}^{4-}$ fragment. Although the $Bi_2X_{10}^{4-}$ fragment has been previously reported in the literature,[8,33−36] $[H_2TMDP]_2[Bi_2Cl_{6.17}I_{3.83}]$ is apparently the first compound containing a mixed-halide $Bi_2X_{10}^{4-}$ anion. In the centrosymmetric, dinuclear anion of **2**, two of the five crystallographically independent halide sites are affected by halide mixing. These sites (Cl3/I3 and Cl4/I4) and those related to them by inversion symmetry (designated "A") are apical ligand sites in relation to the $Bi_2Cl_4I_2$ basal plane. Within the basal plane, two chloride ligands bridge the bismuth centers, and each bismuth center has both a terminal iodide and a terminal chloride ligand. Bond distances and angles for the $Bi_2Cl_{6.17}I_{3.83}^{4-}$ anion are gathered in Table 2.

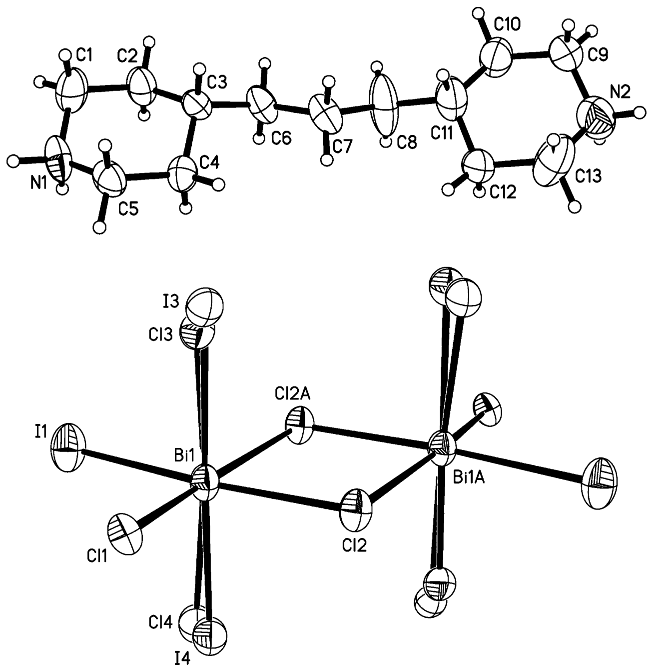

Figure 3. Ellipsoid plots of the components of $[H_2TMDP]_2[Bi_2Cl_{10-x}I_x]$ (**2**, $x = 3.83$) showing the atom labeling scheme. Displacement ellipsoids are drawn at the 30% probability level. The $[H_2TMDP]^{2+}$ cation (top) and the $[Bi_2Cl_{10-x}I_x]^{4-}$ anion (bottom) are shown.

Table 4. Hydrogen Bond Distances (Å) and Angles (deg) for **2**

D−H···A	*d*(D−H)	*d*(H···A)	*d*(D···A)	∠(DHA)
N(1)−H(1C)···I(4)[b]	0.90	2.79	3.621(11)	154.6
N(1)−H(1C)···Cl(4)[b]	0.90	2.81	3.65(4)	155.7
N(1)−H(1D)···Cl(3)[c]	0.90	2.60	3.348(19)	141.3
N(1)−H(1D)···I(3)[c]	0.90	2.79	3.45(2)	131.6
N(1)−H(1D)···I(1)[c]	0.90	3.19	3.818(9)	129.0
N(2)−H(2C)···I(3)[a]	0.90	2.82	3.51(2)	134.4
N(2)−H(2C)···I(4)[d]	0.90	3.22	3.711(13)	116.7
N(2)−H(2D)···Cl(3)[e]	0.90	2.64	3.50(2)	161.1
N(2)−H(2D)···I(3)[e]	0.90	2.76	3.58(2)	151.5

[a−e] Symmetry transformations used to generate equivalent atoms: [a] $-x, -y + 1, -z$ [b] $-x + 1, y - 1/2, -z + 1/2$ [c] $-x + 1, -y + 1, -z + 1$ [d] $-x, y - 1/2, -z - 1/2$ [e] $x, -y + 1/2, z - 1/2$.

As in **1**, several cation−anion hydrogen bonding interactions serve to direct the crystal packing; the details of these hydrogen bonding interactions are summarized in Table 4. However, no halide−halide interactions were observed for the compound. A view of the crystal packing in **2** is shown in Figure 4, where it can be seen that the discrete $Bi_2X_{10}^{4-}$ fragments line up along the (001) unit cell direction.

3.2.3. Compound 3 ($x = 0.99$). $[H_2TMDP][BiBr_{5-x}I_x]$ (**3**, $x = 0.99$) crystallizes in the acentric space group $P2_12_12_1$ and is composed of protonated TMDP cations and polymeric $(BiBr_{4.01}I_{0.99})^{2-}$ anions (Figure 5). The polymeric anion consists of cis corner-sharing BiX_6 distorted octahedral units resulting in the formation of zigzag anionic chains that run along the crystallographic (100) direction. The BiX_5^{2-} zigzag chain motif has been observed in several other halobismuthate materials,[16,37] although this is the first report of such a compound containing a polymeric, mixed haloanion. Of the five crystallographically independent halide sites in the anion, three are affected by halide mixing. These halide sites (I1/Br11, I2/Br22, and I3/Br33) are arranged facially and are located on the outside of the zigzag bends of the chains.

---

(31) Bondi, A. *J. Phys. Chem.* **1964**, *68*, 441.

(32) Shriver, D. F.; Atkins, P. W. *Inorganic Chemistry*, 3rd ed.; W.H. Freeman and Company: New York, 1999.

(33) Chaabouni, S.; Kamoun, S.; Jaud, J. *J. Chem. Crystallogr.* **1998**, *28*, 209.

(34) Charmant, J. P. H.; Norman, N. C.; Starbuck, J. *Acta Crystallogr., Sect. E* **2002**, *58*, m144.

(35) Benetollo, F.; Bombieri, G.; Del Pra, A.; Alonzo, G.; Bertazzi, N. *Inorg. Chim. Acta* **2001**, *319*, 49.

(36) Bowmaker, G. A.; Junk, P. C.; Lee, A. M.; Skelton, B. W. *Aust. J. Chem.* **1998**, *51*, 293.

(37) Mitzi, D. B.; Brock, P. *Inorg. Chem.* **2001**, *40*, 2096.

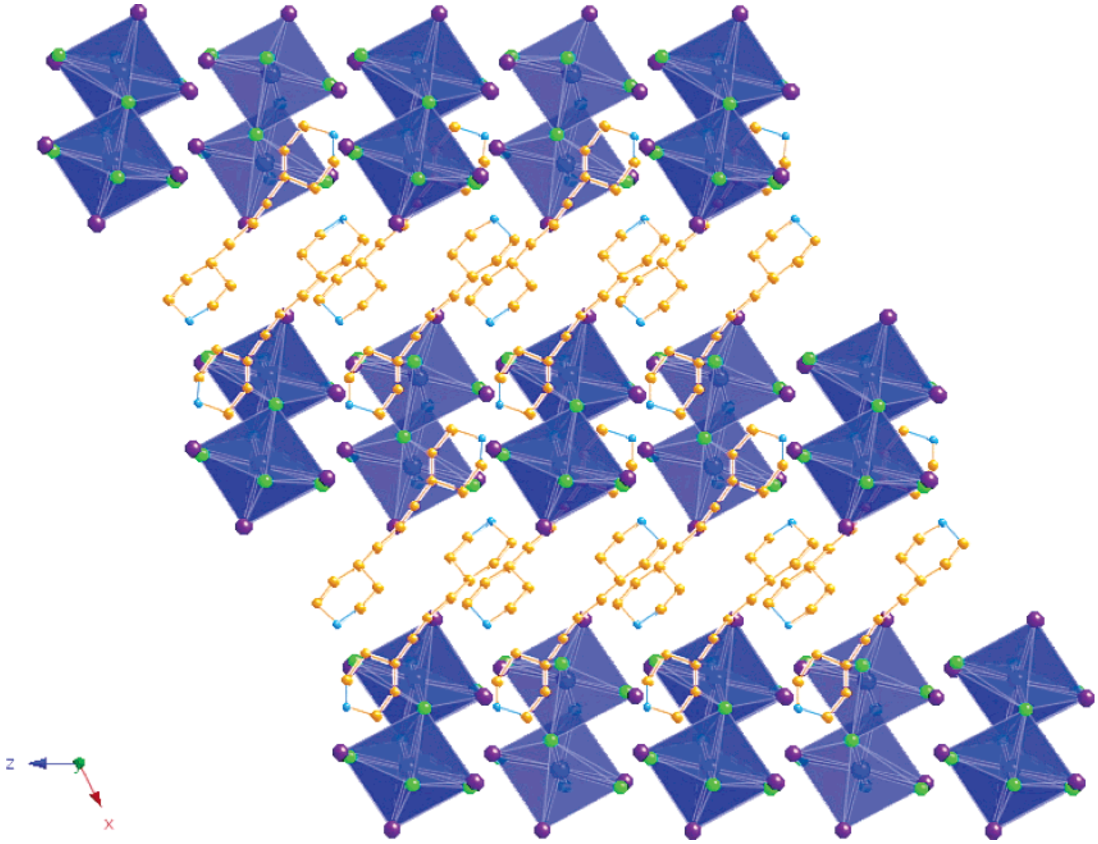

Figure 4. (010) view of the crystal packing in $[H_2TMDP]_2[Bi_2Cl_{10-x}I_x]$ (**2**, $x = 3.83$). Bi polyhedra are shown in blue; Cl, green spheres; I, purple; N, light blue; C, gold. H atoms are not shown.

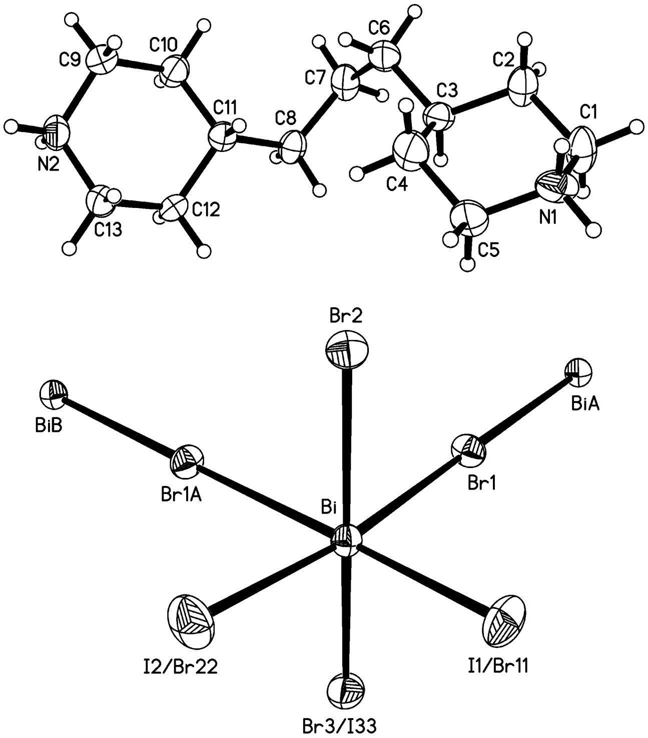

Figure 5. Ellipsoid plots of the cation and anion of $[H_2TMDP][BiBr_{5-x}I_x]$ (**3**) showing the atom labeling scheme. Displacement ellipsoids are drawn at the 30% probability level. The $[H_2TMDP]^{2+}$ cation (top) and the $[BiBr_{5-x}I_x]^{2-}$ anion (bottom) are shown.

Table 5. Hydrogen Bond Distances (Å) and Angles (deg) for **3**

D−H···A	*d*(D−H)	*d*(H···A)	*d*(D···A)	∠(DHA)
N(1)−H(1D)···I(33)[a]	0.90	2.74	3.516(7)	144.5
N(1)−H(1D)···Br(1)[a]	0.90	2.92	3.499(6)	123.4
N(1)−H(1C)···Br(2)[b]	0.90	2.68	3.445(7)	143.7
N(2)−H(2C)···Br(2)[c]	0.90	2.68	3.425(6)	140.7
N(2)−H(2C)···Br(1)[c]	0.90	2.88	3.497(6)	126.9
N(2)−H(2D)···I(33)[d]	0.90	2.64	3.417(6)	145.3

[a−d] Symmetry transformations used to generate equivalent atoms: [a] $x - {}^1/_2, -y + {}^3/_2, -z + 1$ [b] $x + {}^1/_2, -y + {}^3/_2, -z + 1$ [c] $-x + {}^1/_2, -y + 1, z + {}^1/_2$ [d] $-x, y - {}^1/_2, -z + {}^3/_2$.

The remaining terminal halide site and the bridging halide site are occupied solely by bromide ligands. An isostructural compound with $x = 1.70$ was also characterized by single-crystal X-ray diffraction (see Supporting Information) where it was determined that the same three sites were affected by halide mixing. Bond distances and angles for the anionic component of **3** ($x = 0.99$) are given in Table 2.

The crystal packing in **3** is shown in Figure 6 where it can be seen that the inorganic chains are separated by rows of organic cations. As in **1** and **2**, a network of cation−anion hydrogen bonding interactions is responsible for the arrangement of components in the solid; however, no short halide−halide interactions were identified for **3**. Details of the hydrogen bonding interactions present in **3** are listed in Table 5.

3.3. Optical Properties. Diffuse reflectance optical absorption spectra (Figure 7) were collected on pure samples of compounds **1** and **3**. As observed in spectra of related compounds,[5,7] these spectra reveal an excitonic peak followed by a continuum absorbance at higher energy. For **1**, the excitonic band is observed at approximately 477 nm, and

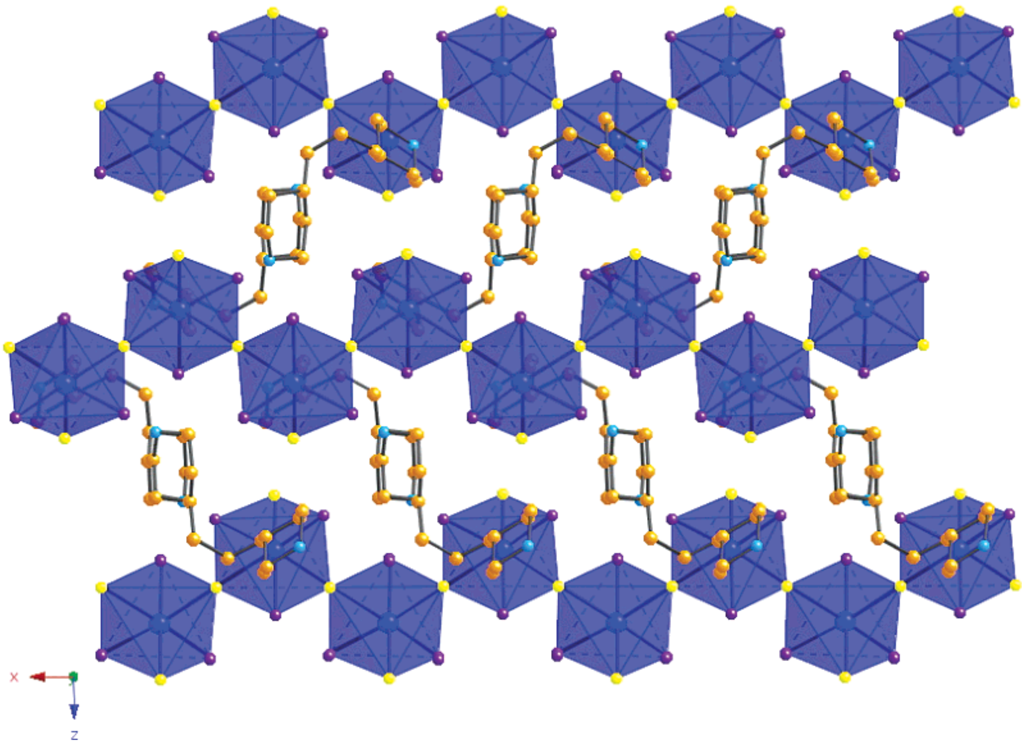

Figure 6. (010) view of the crystal packing in [H_2TMDP][$BiBr_{5-x}I_x$] (**3**). Bi polyhedra are shown in blue; Br, yellow spheres; N, light blue; C, gold. H atoms are not shown. Sites affected by Br/I mixing are shown in purple.

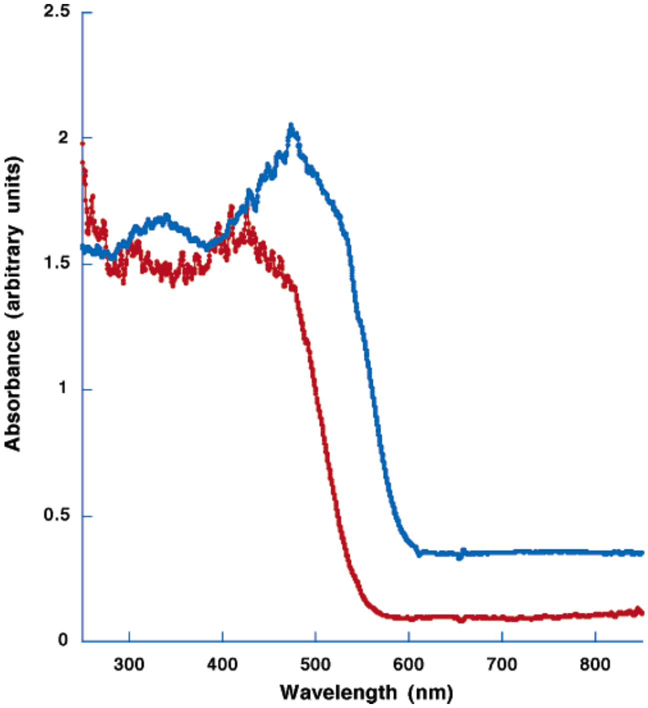

Figure 7. Diffuse reflectance UV−visible absorption spectra for [H_2-TMDP]$_2$[(Bi_2I_9)($BiCl_2I_2$)] (**1**) (blue) and [H_2TMDP][$BiBr_{5-x}I_x$] (**3**) (red) taken at room temperature.

estimating that the continuum absorption begins at the dip following this peak, the band gap energy of **1** is approximately 3.0 eV. A simple, two-probe-conductivity measurement confirmed the poor electrical conductivity of **1**, consistent with the large band gap. For **3**, the excitonic band occurs at about 420 nm, and the continuum absorbance edge corresponds to a band gap energy of approximately 3.5 eV.

Conclusions

While a number of halobismuthate materials have been synthesized and structurally characterized, materials containing mixed haloanions of bismuth are comparatively rare. Herein, we have described a facile solvothermal approach for the preparation of such materials via the reaction of an alkylamine cation source and BiI_3 in the presence of HX, where X = Cl or Br. We anticipate that this approach is extendable to other group 15 trihalides by reaction of MX_3 and an alkylamine with HY, where X and Y are halogens and X ≠ Y. Such materials are likely to exhibit interesting optical and electronic properties and, in addition, may be useful for understanding certain synthetic organic transformations, such as transhalogenation reactions. Current synthetic efforts are directed at the preparation of mixed-metal halobismuthate materials, as such materials may also exhibit interesting optical, electronic, or even magnetic properties resulting from the synergistic interaction of different metal centers. This effort has yielded promising preliminary results which will be reported shortly.

Acknowledgment. Financial support was provided by the National Science Foundation through Grant Numbers CHE: 0314164 and CHE:0315152.

Supporting Information Available: Listings of atomic coordinates and equivalent isotropic displacement parameters for **1**, **2**, and **3** (x = 0.99 and x = 1.70). Table detailing halide−halide interactions for **1**. Crystallographic information in CIF format for **1**, **2**, and **3** (x = 0.99 and x = 1.70). This material is available free of charge via the Internet at http://pubs.acs.org.

IC049212D